

Hydraulic Analogy Study of Supersonic Rectangular-Jet Screech Control with Cylinders

Anthony Buchanan, Rowan Macartney, and Mark C. Thompson
Monash University, Clayton, Victoria 3800, Australia
Eric Brocher
Institut de Mécanique des Fluides de Trets, 13530 Trets, France
and
Kerry Hourigan*
Monash University, Clayton, Victoria 3800, Australia

DOI: 10.2514/1.26714

An investigation into the control of the screech noise of two-dimensional underexpanded supersonic jets was carried out using the hydraulic analogy. Favorable agreement was found with previous experiments between the variations with pressure ratio of the measured screech-amplitude variation and the screech frequency. Remarkably, the intensity of the screech tone was able to be altered substantially by the positioning of a relatively small cylinder along the centerline of the jet flow. Two different cylinder diameters and two different Froude (Mach) numbers were tested. The normalized change in screech-tone intensity for all cases was found to correlate with the relative position in the shock cell of the intersection of the cylinder bow wave and the jet shear layer.

Nomenclature

a_g	= speed of sound, $m \cdot s^{-1}$
a_w	= speed of water waves, \sqrt{gh} , $m \cdot s^{-1}$
c	= distance from the end of the first shock cell to the cylinder wake along the shear layer, m
d	= cylinder diameter, m
Fr	= dimensionless Froude number, U_0/a_w
f	= screech-tone frequency, Hz
g	= gravitational constant, $m \cdot s^{-2}$
h	= local water depth, m
h_0	= mean water depth, m
I	= screech acoustic intensity, $W \cdot m^{-2}$
I_0	= screech acoustic intensity (free jet, no cylinder in wake), $W \cdot m^{-2}$
L	= shock-cell length (with cylinder in wake), m
L_{no}	= shock-cell length (free jet, no cylinder in wake), m
Ma	= dimensionless Mach number, U_0/a_g
p	= fluid pressure, Pa
p_a	= acoustic pressure (rms), Pa
$p_{a,max}$	= maximum acoustic pressure (rms), Pa
p_o	= ambient fluid pressure, Pa
R	= dimensionless pressure ratio (across nozzle)
Re	= dimensionless Reynolds number, $U_0 w / \nu$
St	= dimensionless screech Strouhal number, $f w / U_0$
T	= fluid temperature, K
T_0	= ambient fluid temperature, K
U_0	= jet velocity at nozzle exit, $m \cdot s^{-1}$
u	= axial fluid velocity, $m \cdot s^{-1}$
v	= lateral fluid velocity, $m \cdot s^{-1}$
w	= jet nozzle width, m
x	= distance along the jet axis from the nozzle exit, m

y	= distance from the center of the nozzle exit, lateral to the jet axis, m
γ	= dimensionless ratio of specific heats
ν	= kinematic viscosity, $m^2 \cdot s^{-1}$
ρ	= fluid density, $kg \cdot m^{-3}$
ρ_0	= ambient fluid density, $kg \cdot m^{-3}$

Introduction

SINCE the pioneering research of Powell [1], many theoretical and experimental investigations have been undertaken into the aeroacoustic phenomenon of screech, including Ho and Nosseir [2], Tam [3], Brocher and Makhsud [4], Panda [5], Alkislar et al. [6], and Norum [7].

Tam [3] identifies three shock-associated noise components associated with an imperfectly expanded supersonic jet: namely, turbulent mixing noise, broadband shock-associated noise, and screech tones. In such a jet, a dominant discrete frequency with a sound pressure level greater than all other noise components can appear. This is referred to as the fundamental screech tone, and is often accompanied by its harmonics.

Powell [1] proposed an elementary theory of screech generation, based upon the hypothesis that the acoustic energy originates from the interaction of the stream disturbances with the radiated sound. Powell's conception describes a feedback loop in which a disturbance in the shear layer of the jet creates a sound wave as this disturbance traverses across a shock cell, with this interaction effectively behaving as an acoustic source. This theory was refined over the last half-century, with the Alkislar et al. [6] description suggesting that this sound wave propagates upstream in the ambient medium and creates a stream disturbance in the immediate neighborhood of the jet exit by interacting with the incipient shear. This disturbance continues downstream with the jet until it again traverses the source and a sound wave is produced. The sound wave travels in the upstream direction adjacent to the jet and applies a localized pressure force at the nozzle exit, which excites the shear layer, thus completing the feedback loop. This feedback concept assumes that the sound waves are of sufficient strength to govern the stability of the boundary of the stream close to the nozzle exit. Powell [1] suggests that these periodic disturbances in the shear layer of the jet will become amplified with increasing downstream distance until significant acoustic energy can be produced as the disturbance traverses a shock cell.

Received 23 July 2006; revision received 28 November 2006; accepted for publication 21 March 2007. Copyright © 2007 by the American Institute of Aeronautics and Astronautics, Inc. All rights reserved. Copies of this paper may be made for personal or internal use, on condition that the copier pay the \$10.00 per-copy fee to the Copyright Clearance Center, Inc., 222 Rosewood Drive, Danvers, MA 01923; include the code 0001-1452/07 \$10.00 in correspondence with the CCC.

*Professor, Fluids Laboratory for Aeronautical and Industrial Research (FLAIR), Department of Mechanical Engineering, Clayton Campus; kerry.hourigan@eng.monash.edu.au (Corresponding Author).

This feedback loop is consequently liable to set up a resonance phenomenon that leads to a self-sustained oscillatory condition that Alkislar et al. [6] state is common to nonideally expanded jets. Hence, resonance of acoustic waves at a discrete frequency will lead to a single dominant aeroacoustic noise source.

Multiple researchers, including Powell [1] and Panda [5], developed models to predict screech frequency. For example, Panda discussed the previously traditional argument that the average shock spacing of the characteristic shock train of the plume of an imperfectly expanded supersonic jet is the primary length scale governing the screech phenomenon and its frequency. He suggests that the primary length scale is in fact the standing wavelength, described as the distance between the node points in the interference pattern formed by the hydrodynamic and acoustic waves. This contention is supported by experimental results obtained in a free-air-jet facility.

Panda [5] also provided guidance as to obtaining clear experimental measurements of the screech intensity. He stated that along the jet boundary, the hydrodynamic fluctuations are found to be an order of magnitude higher than the acoustic fluctuations, but that they decay exponentially away from the jet boundary. Hence, the acoustic fluctuations evidently dominate after a certain radial distance from the source, indicating that measurements of screech tones should be carried out in the far field of the jet. In the present experiments, the water surface fluctuations, analogous to the acoustic waves in air-jet experiments, were measured several jet diameters laterally away from the jet exit, for which Fig. 5 of Panda [5] shows that the rms pressure fluctuations are locally significant but fairly uniform spatially. That is, along a line lateral to the jet exit, the sensor is far enough away to avoid the turbulent jet shear layers and to record sharp spectra for the screech-line tones, as will be seen in the present study.

The development of accurate prediction models for screech intensity, however, has thus far been elusive. Brocher and Makhsud [4] performed their study on a water table through application of the hydraulic analogy between water flow with a free surface and two-dimensional compressible gas flow. They propose that the screech intensity does not depend on the shock strength itself, but rather on the value of the local pressure gradient at the periphery of the jet, just upstream of the source. This is consistent with the observation that the screech intensity drops off significantly beyond a certain Mach number, even though strong shock cells are still observed. Brocher and Makhsud suggested that the kinetic energy in the shear layer is unable to overcome the pressure gradient at the source and will therefore undergo a lateral deflection and form a vortex; hence, the stronger the gradient, the larger the vortex. These vortices then couple with the flow velocity and the acoustic velocity of the jet and generate acoustic power at the screech frequency.

Alkislar et al. [6] attempted to refine the link between the screech-tone intensity and the static pressure gradient at the location of screech-sound generation. Their results indicated that intense sound was generated when large-scale spanwise vortices interacted with the compression regions of the shock cell of interest (the acoustic-wave source), and that the strength of these vortices is likely to play a significant role in determining the screech-tone intensity. Alkislar et al. also suggested that suppression of the mechanism generating these large-scale structures may result in turbulence suppression and therefore lead to reductions in the far-field noise. This provides an indication of the direction of future research into screech control and damping techniques.

However, despite a current lack of a complete understanding of the physical mechanisms governing screech-tone generation, a number of researchers have performed experimental analyses of a variety of screech-control methods based on present knowledge of these processes, testing their viability as potential techniques of screech suppression.

Norum [7] investigated the effect of varying the nozzle-exit geometry on the feedback process inherent to screech production on the basis that this process involves an interaction between the generated screech waves (acoustic waves) with the nozzle exit. He concluded that small modifications to the external surface of the

nozzle at the jet exit had a large effect on the strength of the screech process. He observed reductions in screech amplitudes with decreasing lip thickness and the introduction of small protrusions, or tabs, into the jet at the nozzle lip. Norum also found that modifications to the internal surface of the jet nozzle produced favorable results, with large slots in the nozzle exit yielding extensive suppression of screech tones. However, the effect such modifications may have on the ability of the nozzle to produce thrust was not considered.

Nagel et al. [8] used a sound-reflecting surface positioned upstream of the nozzle exit. The objective of this device was to establish a standing-wave pattern of acoustic waves with a node at the nozzle-exit plane, thereby destroying the feedback process associated with screech-tone generation. They found that nonintrusive tabs at the nozzle exit are capable of achieving limited screech-amplitude reduction, whereas intrusive tabs have proved more useful in screech-tone elimination but result in a severe distortion of the flow and a thrust penalty. This screech cancellation could effectively be achieved with the reflecting surface at distances of one-quarter of the screech wavelength, three-quarters of this wavelength, and so on, from the nozzle exit. In the present experiments, the aim is to modify or add to the sound sources, rather than to introduce a reflective surface, to attenuate the screech tone.

Umeda et al. [9] investigated experimentally the discrete tones generated from high subsonic and choked underexpanded jets of air using a circular nozzle. A slender circular cylinder was placed across the jet, and it was found that an impinging tone resulted for nozzle-to-cylinder distances less than eight nozzle diameters. The results suggested that there is an analogy between the resonance mechanisms for the discrete tones of the screech and the impinging tone produced by the cylinder, which was visualized using the schlieren technique.

In this paper, we investigate the control of the screech noise of two-dimensional underexpanded supersonic jets using the hydraulic analogy. First, the characteristics of the free-jet screech are validated against previous air- and water-table results. Then, the effect on the screech tone by placing a cylinder along the centerline of the jet flow is investigated in detail. In the experiments of Umeda et al. [9], the jet was round and the cylinder was placed across the jet diameter, extending through and well beyond the shear layers. However, in the present experiments, the jet was two-dimensional (rectangular) and the cylinder was placed, with its axis spanwise, on the centerline of the jet, therefore not piercing the jet shear layer. The amount of attenuation and amplification of the screech noise will be shown to correlate well with the position, relative to the shock cells, of the cylinder bow shock intersection with the jet shear layer.

Hydraulic Analogy

The hydraulic analogy states that a shallow water flow is analogous to a two-dimensional compressible ideal gas flow, in which changes in pressure, temperature, and density correspond to changes in water height (Preiswerk [10]). Table 1 summarizes the hydraulic analogy. In particular, the analogy is useful for simulating high-speed jet flows, as demonstrated using a water table by Brocher and Makhsud [4]. The experiments in the analogy are relatively simple, low-cost, and low-energy to construct and run. Also, the water-height fluctuations can be easily measured accurately using nonintrusive techniques such as the optical photonic sensor. The relative wave and flow speed is three orders of magnitude slower than that of a gas flow, further increasing the accuracy and ease of visualization on the water table.

Table 1 Analogous equations and variables for two-dimensional gas and shallow hydraulic flows

Gas flow	Hydraulic flow	Implication
$\frac{T}{T_0} = 1 + \frac{\gamma-1}{2} Ma^2$	$\frac{h}{h_0} = 1 + \frac{1}{2} Fr^2$	$\frac{T}{T_0} \equiv \frac{h}{h_0}, \gamma = 2$
$\frac{\partial}{\partial x}(\rho u) + \frac{\partial}{\partial y}(\rho v) = 0$	$\frac{\partial}{\partial x}(hu) + \frac{\partial}{\partial y}(hv) = 0$	$Ma \equiv Fr, \frac{\rho}{\rho_0} \equiv \frac{h}{h_0}$
$\frac{p}{p_0} = \frac{\rho}{\rho_0} \frac{T}{T_0}$		$\frac{p}{p_0} = \left(\frac{h}{h_0}\right)^2$

The analogy does not provide a direct quantitative representation of aerodynamic flows in air, but rather that of a hydraulic gas (Black and Mediratta [11]), in which the ratio of specific heats is two. However, De Chant and Caton [12] stated that this classical limitation of the hydraulic analogy is less restrictive if the analogy is describing flows in which there is likely to be a limited effect resulting from varying specific heat ratios. This is supported by Brocher and Makhsud [4], who suggested that this is not of particular importance because relevant experiments with gases have shown no important influence of γ .

To achieve dynamic similarity between the two wave propagations, the ratio of the freestream velocity to the wave-propagation velocity is used as an analogous nondimensional property when describing the flow. These ratios are the Froude number in water (in which the representative length is the local water depth) and the Mach number in a gas.

De Chant and Caton [12] provide a useful summary (recreated in Table 1) of these mathematical developments and the implications of the analogous expressions describing the flow of gas and water.

The hydraulic analogy has provided good quantitative comparisons with the equivalent airflows in a range of situations, including the shooting flow around a wedge and around a cylinder [13], the interaction of a cylinder wake with a resonator tube [14], the study of a shock-wave magnetohydrodynamic generator [15], and two-dimensional supersonic jet flows [4,12].

Experimental Setup

Water Table

The water table was designed based on a similar table used by Brocher and Makhsud [4]. A schematic diagram of the water table is shown in Fig. 1.

The bed of the table consists of a horizontal sheet of clear plate glass approximately 16-mm thick, 2000-mm long, and 1410-mm wide. This glass section constitutes the working section of the table and is bounded on its sides by glass walls 16-mm thick and 95-mm high, thus allowing water depths up to 95-mm deep across the test section. A high level of flatness across the span and length of the table bed was deemed essential and was achieved by the installation of appropriate structural support beneath the glass to ensure that the maximum deflection does not exceed 0.1 mm.

Upstream of the test bed, a supply reservoir provides the source for water flow across the table. Downstream of the glass section, the table is fitted with a beach, 600 mm in length, angled upwards relative to the horizontal. This angle dictates the downstream water-depth conditions present on the table and is variable through the adjustment of its supporting screws, allowing a desired downstream water depth to be maintained during the experiment. A downstream reservoir was

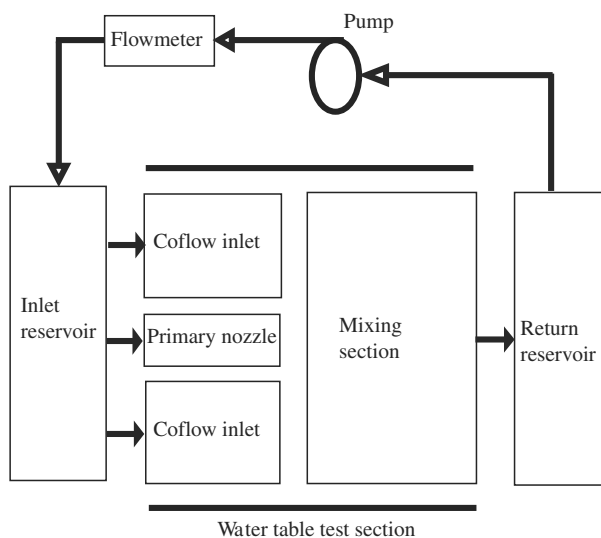


Fig. 1 Schematic diagram of the water table.

not filled but contained enough water to minimize the development of bubbles as the water exited the test section of the table and flowed into the stored water in the downstream reservoir. Both reservoirs have capacities of approximately 500 liters.

The water is returned from the downstream reservoir to the upstream reservoir by a small 1.5-kW centrifugal pump driven by a 2-kW dc motor. The pumping system consists of a feedback control system that employs a magnetohydrodynamic flowmeter to provide continuous monitoring of the pump volumetric flow-rate output and thereby maintain a constant flow into the upstream reservoir.

To lessen the surging and turbulence induced by the inflow of water into the upstream reservoir, the water is injected through a 100-mm layer of small river rocks. The level of water in the upstream reservoir effectively determines the volumetric flow rate across the test section of the table for any given experimental setup. This water level is controlled directly by adjusting the pump output to raise or lower this water level. Importantly, the feedback-control system across this pump allows consistent and repeatable experimental conditions.

Along the side walls of the table test section, a method similar to that employed by Brocher and Makhsud [4] (that is, the placement of foam rubber with a series of triangular cutouts) was used to damp transverse waves generated by the jet throughout the length of its shock train. Steel wool proved to provide an effective damping solution to high-frequency wave and noise generation along the upstream boundary of the nozzle walls; however, it only demonstrated a limited effect on the generation of low-frequency longitudinal standing waves.

Measuring Apparatus and Computational Results Analysis

A sensing system, similar to that employed by Brocher and Makhsud [4], using optical fiber photonic sensors was chosen on the basis of evidence supporting its suitability to this application in sensing small and frequent oscillations or fluctuations in the position of a surface analogy.

The MTI-2000 Fotonic Sensor is a dual-channel, optical-fiber system that performs noncontact displacement and vibration measurements. The sensor allows nonintrusive measurements of fluctuations in the position of the free surface for any given location across the water table using fiber-optic probes.

A sampling rate of 200 measurements per second across a suitable sampling time was sufficient to provide useful and relevant information for the purpose of this research. These raw data were recorded on a computer. Analysis was performed by a LabView program, which performed noise reduction, Fourier frequency and amplitude analysis, and filtering to provide a graphical output displaying the wave amplitude or intensity as a function of the frequency of that wave in the form of a frequency spectrum.

Nozzle

The nozzle was designed to match the N1 nozzle used by Brocher and Makhsud [4] (several similar experiments have been carried out elsewhere in air [16]), taking the form of a converging nozzle (see Fig. 2). Although some variations exist for differently shaped nozzles, the main characteristics of the screech tone are similar and

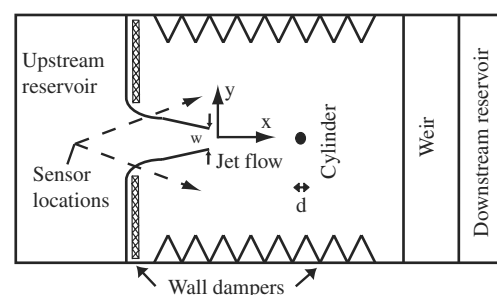


Fig. 2 Schematic of the experiment.

comparison can be made across a range of nozzle geometries and operating conditions, for example, as presented by Lebedev [17].

The walls of the converging nozzle consisted of parallel walls 135 mm apart, extending a distance of approximately 90 mm, followed by walls converging at a half-angle of approximately 5 deg, for a length of 441 mm. The nozzle-exit width was 57 mm, with a nozzle-exit lip thickness tapered to approximately 1.5 mm. This lip thickness was minimized to prevent amplification of the screech-wave-generation process (Norum [7] and Nagel et al. [8]). For these experimental conditions, the Reynolds number of the jet was of the order of 5×10^4 , thereby resulting in turbulent shear layers and large-scale structures that were observed to convect at approximately $0.6U_0$, similar to that found in gas jets.

For a jet, the relationship between the pressure ratio and the Mach number in a compressible gas is given by White [18] as

$$\frac{p}{p_0} = \left[1 + \frac{1}{2}(\gamma - 1)Ma^2 \right]^{\frac{\gamma}{\gamma - 1}} \quad (1)$$

Table 1 shows the relationship between the pressure ratio and the water-height ratio used when applying the hydraulic analogy. To achieve supercritical flow (the hydraulic analog of supersonic flow) from the nozzle exit, at least for parallel jets, the water-height ratio between the upstream and ambient downstream regions of the flow must be equal to or greater than 1.5, or equivalently, the pressure ratio must exceed 2.25.

The nozzle was mounted in the center of two walls that spanned the remaining width of the table. These walls provided the necessary flow restriction to obtain a deeper upstream water height than that of the ambient flow downstream of the nozzle, thus inducing a pressure ratio across the nozzle. These walls, aligned perpendicularly to the side walls of the test section of the water table, were manufactured to a height of approximately 95 mm, allowing an equivalent maximum water depth upstream of the nozzle. The 90-deg transition between these walls and the nozzle walls was achieved gradually with the use of corners rounded to a radius of curvature of approximately 50 mm. The flow-restriction walls were also modified to allow limited coflow into the ambient mixing section of the table around the nozzle. These walls and its associated modifications are shown in Fig. 2. The flow-restriction walls and both the parallel and contracting sections of the nozzle were laid on the glass surface of the test section of the water table. Tape or a temporary sealant was used to prevent leakage between the two perpendicular surfaces.

A two-dimensional Cartesian coordinate system, (x - y), was used to describe the selected locations both downstream and upstream of the nozzle exit at which measurements were performed. This coordinate system was selected with its origin located at the center of the nozzle-exit plane, with the x axis oriented along the centerline of the jet and the y axis perpendicular to this centerline, and is shown in Fig. 2.

Data Acquisition and Postprocessing

The measurements performed here were conducted with a constant downstream water height of 27 mm, whereas the nozzle depth ratio (and hence pressure ratio, as defined by Table 1) was varied by changing the upstream water depth using the pump control and flowmeter. This water level was chosen after testing for a range of levels as providing a clearly defined jet and shock cells, consistent with the reported equivalent air experiments. It should be noted that the jet structure was not sensitive over a fairly wide range of water-level heights. Although a water-level height for nondispersion of wave frequencies is somewhat lower, our concentration here is on the screech tone and not the relative wave speeds. The measurements were again taken at a location defined by $x/w = 0$ and $y/w = 3$ with respect to the nozzle-exit plane and coordinate system defined in Fig. 2. A sampling time of 1500 s was used during data acquisition, and a coflow of 5.6% was maintained throughout the ambient region surrounding the jet. A range of coflows across the table, which occur naturally adjacent to a jet because of the Venturi effect, was considered: the value chosen was to be relatively small but providing

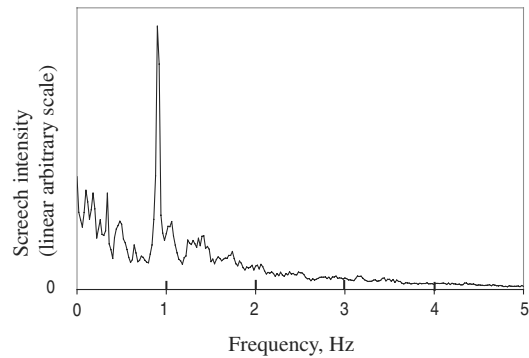


Fig. 3 Typical frequency spectrum ($Fr = 1.51$, free jet).

a stable jet structure. Above a coflow of 5%, to the maximum measured, 10%, the jet structure and screech characteristics were insensitive to the actual value.

The resulting data were in the form of frequency spectra, corresponding to each pressure ratio at which the nozzle was operated, allowing identification of screech tones and their associated frequency and amplitude.

An example of such a frequency spectrum is shown in Fig. 3, corresponding to a Froude number of 1.51. Clearly seen is a prominent peak in sound intensity at approximately 1 Hz, representing a distinct screech tone.

Visualization

A shadowgraph system was used, in which a uniform parallel light source above the table was directed down, normal to the uneven water surface. The refraction of the water surface leads to lighter and darker areas (shadows) being cast on a semitransparent screen placed as close as possible underneath the glass floor of the table. A camera was placed some distance below the screen to take photos of the shadow cast on the screen, and clear images were obtained. The visualization images shown throughout this section were taken with relatively long exposures, 15 to 30 s, which equated to anywhere from 15 to 60 periods of the screech-generation cycle. It became necessary to use these long exposures because the time-dependent nature of the jet meant that a regular exposure photo, taken at a split second in time, would not be an adequate representation of the feedback system. The advantages of the long exposure were that a time-averaged picture of the flow was produced from which the shock-cell pattern was clear.

Results and Discussion

First, the screech characteristics, such as the variation of screech-tone intensity and frequency as a function of Froude number or pressure ratio, of the supercritical jet using the N1 nozzle will be presented. Then the effect of placing cylinders of different diameters along the wake centerline is shown, and the mechanism for the periodically varying amplification/attenuation of the screech-tone intensity is discussed.

Screech-Tone Characteristics and Behavior of the Free Jet

The plot of Fig. 4 shows the normalized screech amplitude as a function of the nozzle pressure ratio, with a peak found at a pressure ratio of 4. Although some differences are present due to different rig and nozzle setups, the variation is similar to that measured by Krothapalli et al. [19] with air using a parallel-flow rectangular jet and by Brocher and Makhsud [4] using type N1 and N2 converging nozzles on a water table.

Although the measured screech frequencies in water exist at considerably smaller magnitude than generally found in air, it is still possible to make a general comparison of the measured data by using the nondimensional Strouhal number. The Strouhal number variation with pressure ratio for the experimental data obtained in this study was again plotted against similar data obtained by Brocher

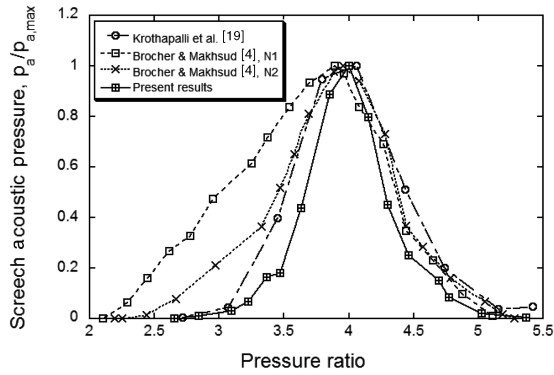


Fig. 4 Normalized variation of the screech acoustic pressure and comparison with previous results.

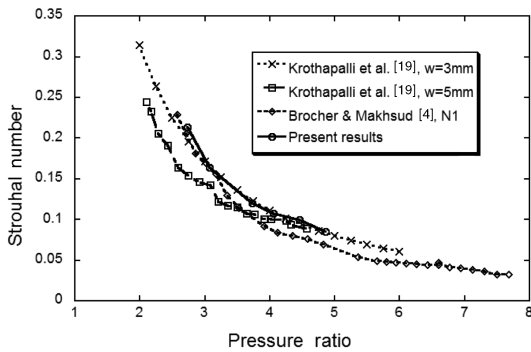


Fig. 5 Variation in the Strouhal number with the pressure ratio.

and Makhsud [4] and Krothapalli et al. [19] (shown in Fig. 5). A slight staging in the Strouhal number of the experimental data obtained in this study at pressure ratios of approximately 3.5 and 4.5 can be observed, corresponding to changes in the dominant screech tone. A close similarity was found to the data obtained by Brocher and Makhsud and Krothapalli et al., particularly at pressure ratios above approximately 3.5.

Cylinder in the Jet

The preceding and various other common measurements of the shock cells, such as their length as a function of Froude number, both on the present rig and by Brocher and Makhsud [4], have produced results of the screech tone in line with those obtained in air by various authors. The next stage was to alter the screech tone by placing cylinders at varying positions along the jet centerline. These experiments were intended to further investigate the factors that control the intensity of the screech tone, as well as providing some insight into possible screech-reduction techniques.

Brocher and Makhsud [4] described the screech intensity as being linked to the local pressure gradient at the end of the second shock cell. It was reasoned in the current experiments that if either the strength, stability, or position of the shock cells could be changed or a new shock introduced, then the screech intensity could possibly be altered. Hence, cylinders of different diameters were placed along the centerline of the jet to achieve these changes in the shock cells. By considering which shock-cell changes correspond to the maximum changes in the screech tone, it could be possible to draw certain conclusions as to the nature of the feedback loop that produces a screech tone. Figure 6 shows a diagram of the experimental setup.

Two cylinder diameter ratios were tested: $d = 2$ and 4 mm or $d/w = 0.035$ and 0.07 , each for two Froude numbers, $Fr = 1.25$ and 1.51 . These two Froude numbers are representative of the range in which the screech intensity is significant and the shock cells are well established, but lower than the value (approximately 1.65) at which the screech tone becomes unsteady [20]. The cylinder

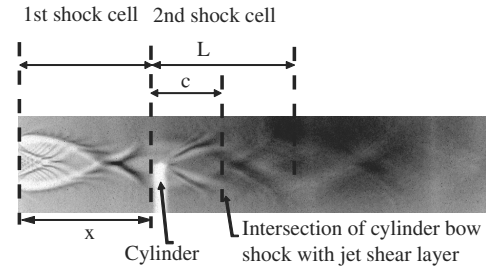


Fig. 6 Schematic of dimensions for the jet with a cylinder.

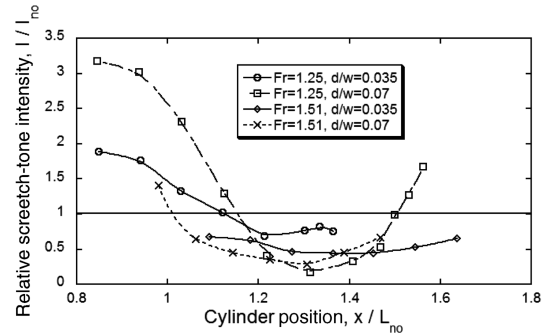


Fig. 7 Screech-tone intensity variation, normalized to that of the free jet at the same Froude number, with cylinder position.

diameters were chosen because they are relatively small compared with the nozzle diameter, did not significantly disturb the shock-cell structures, and were readily available. A larger diameter cylinder, $d = 8$ mm, was found to significantly disturb the shock cells downstream. A set of visualization images and water-height time-series sets were taken with the cylinder placed at various distances downstream of the nozzle exit on the centerline of the jet.

Figure 7 shows the variation in screech-tone intensity, relative to the free jet for the same Froude number, with cylinder position, nondimensionalized by the free-jet shock-cell length for each diameter and Froude number combination. The variation in screech-tone intensity was greater for the lower Froude number and for the larger cylinder diameter. Depending on the position of the cylinder and the particular cylinder and Froude number, amplification of the screech-tone intensity exceeded three, or reduction to approximately 0.17 occurred. The cylinder was found to be placed in quite different positions in the shock-cell structure to achieve the maximum reduction. Initially, it was hypothesized that vortex shedding from the cylinder may affect the flow structures and resultant screech. However, this outcome suggests that the position of the cylinder itself within the shock-cell structure is not a suitable indicator to predict the screech reduction. Interestingly, in each case, there was very little variation in the screech-tone frequency for cylinder position (see Fig. 8). In fact, these frequencies were almost identical to the free-jet value at the same Froude number. Evidently, the cylinder, being of relatively small dimension, does not alter the relevant dimensions of the flow structures (such as the shock-cell lengths or the standing wavelength proposed by Panda [5]) that are part of the feedback loop and frequency.

As shown by Fig. 7, there was a large change in intensity with cylinder position, which followed a mostly sinusoidal profile. In the case of the larger diameter cylinder ($d/w = 0.07$) and $Fr = 1.25$, the frequency spectra for a free jet and the cylinder positions for maximum and minimum screech-tone intensities are shown in Fig. 8. This figure highlights the change in intensity, with the maximum being found to be over 300% of the free-jet screech-tone intensity. The minimum was barely noticeable above the background noise of the free jet.

The flow visualizations for the case of the smaller-sized cylinder ($d/w = 0.035$) are shown for a Froude number of $Fr = 1.25$ in

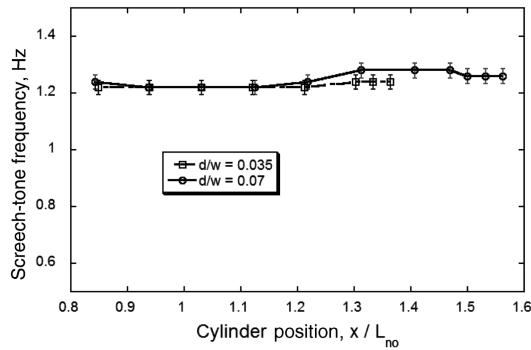


Fig. 8 Screech-tone frequency variation with both cylinder positions relative to shock cells; $Fr = 1.25$.

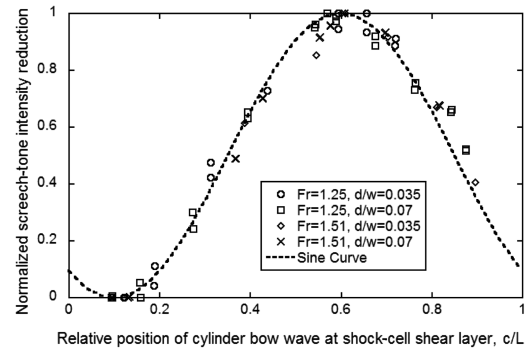


Fig. 10 Normalized screech-tone intensity vs position, relative to the local shock cell in which it resides, at which the cylinder bow shock wave intersects with the jet shear layer.

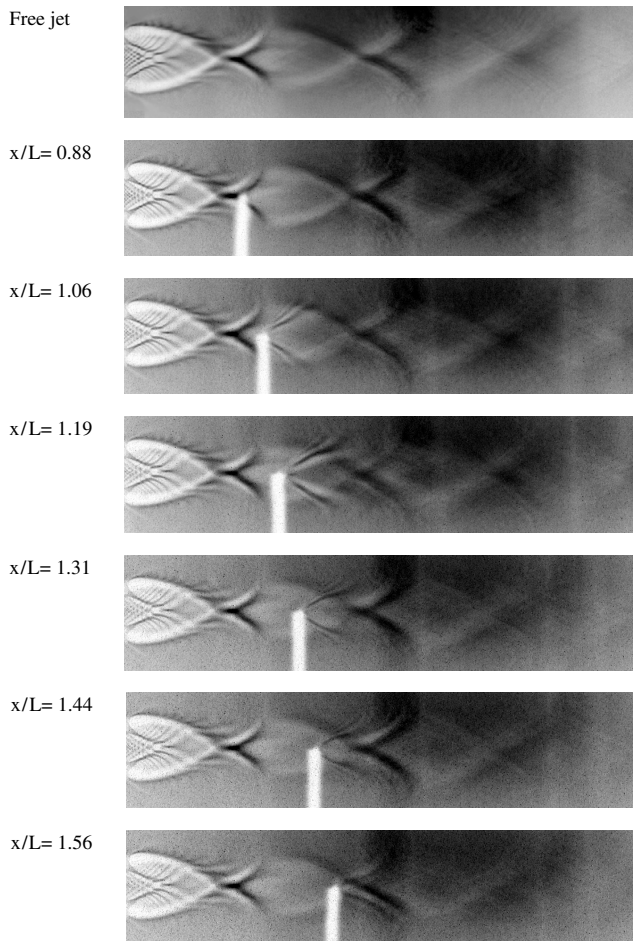


Fig. 9 Visualization images for $Fr = 1.25$ with the smaller cylinder ($d/w = 0.035$) at different normalized distances x/L from the jet exit.

Fig. 9. The cylinder itself generated a bow shock that appeared as a hydraulic jump in the water (the equivalent of a shock wave in air). For most cylinder positions ($x/L = 1.06$ – 1.44), this bow wave is an additional shock intersecting with the jet shear layer. At other cylinder positions ($x/L = 0.88$, 1.56), the bow shock joins the existing shock cells and appears to strengthen the intensity of the shock cell.

An interesting observation is that the cylinder bow wave seems to propagate from the jet centerline at an angle different from that of the hydraulic jumps of the shock cells. This difference in angles could be explained by the local variations in velocity through the jet plume, which can be quite large in magnitude (Brocher and Makhsud [4]). It is also observed that the cylinder bow shock did not have an

observable reflecting hydraulic jump off the shear layer, as seen with the shock-cell hydraulic jumps. The bow shock seemed to disappear as it reached the edge of the supersonic jet, beyond which the flow was relatively low. Despite the strong cylinder bow shock, the existing jet shock-cell structure was unmoved downstream of the cylinder. The second shock cell also appeared to increase in strength when compared with the free-jet case, which would increase the pressure gradient at the end of the second shock cell. This is in strong agreement with the Brocher and Makhsud [4] results, which indicate that screech intensity is proportional to the pressure gradient at the end of the second shock cell.

As known from previous research (e.g., Norum [7]), the frequency of the screech tone is determined by the length of the feedback loop (that is, the distance from the fixed point of receptivity: the exit of the nozzle) to the relevant sound sources in the flow. Evidently, the size of the feedback loop is not changed by cylinder position. The primary upstream propagating-wave-generation point is still the same, despite the extra shock or hydraulic jump, due to the cylinder's presence, that the downstream traveling instability waves must pass.

The generation of screech tone was previously ascribed to the interaction of vorticity waves in the jet shear layer with shock cells, producing acoustic waves that radiate away outside the jet. Part of the wave fronts travel to the receptive region of the jet just downstream of the nozzle to stimulate new vorticity waves that are convected downstream to complete the feedback loop. The visualizations indicate that the presence of the cylinder can produce an additional shock, due to the bow wave, at the jet shear layer with which the vorticity waves can interact. The resulting acoustic waves then attenuate the screech intensity, depending on the relative phase of these acoustic waves relative to the existing screech waves.

However, it was also observed that maximum reduction in screech intensity occurred as the bow shock from the cylinder reached the shear layer about halfway between the two shock cells. Interestingly, this same observation was made for both cylinders at both Froude numbers tested. To further explore this observation, the screech-tone intensity was plotted against the position relative to the local shock cell in which the cylinder bow shock reaches the shear layer (Fig. 10). These dimensions had to be determined from measurements taken on visualization images, which are shown in Fig. 9. The intensities plotted are simply scaled against the difference between maximum and minimum intensities measured for each individual case. Some inaccuracy is involved in determining these distances, on the order of 5%; however, much care was taken and measurement from various images were averaged to obtain each point. For most cases in this plot, the results from the sensors on both sides of the jet are included.

As the plot in Fig. 10 shows, there is a significant collapse of data points when compared with the original plot in Fig. 7, and the variation is approximately sinusoidal. This suggests that the location at which the bow wave of the cylinder reaches the shear layer is of more importance to the screech-tone intensity than the cylinder position itself. Also, it is the relative position in the shock cell, rather than the particular shock cell, that is important. This result is consistent with the hypothesis that by creating a hydraulic jump

180_deg out of phase with the existing shock cells, antinoise is generated through interaction with the shear-layer vorticity waves that are responsible for the original screech tone. Alternatively, the bow wave may be coinciding with a node of the standing wave observed by Panda [5]. Note that the maximum reduction in screech-tone intensity occurs when the bow wave cuts the shear layer at approximately 0.6 of the shock-cell length, which is slightly beyond the expected midpoint position. This may be accounted for by the difference in shear-layer mean velocity, and hence the vorticity-wave velocity, which would be lower in the second half of the shock cell in which there is an adverse pressure gradient.

Conclusions

Control of the screech noise of two-dimensional underexpanded supersonic jets was carried out using the hydraulic analogy. The intensity of the screech tone was able to be altered significantly by placing a cylinder in the jet flow. The amount of reduction and increase was found to correlate with the relative position in a shock cell of the intersection of the cylinder bow shock wave and the jet shear layer. The precise mechanism, speculated to be the addition of another sound source, will be explored in the future through more detailed measurements of the flow pressure and velocity fields using the surface topographic technique [21] and particle image velocimetry. Depending on the position of the cylinder bow shock, additional screech sound can be produced to augment or attenuate the original screech. Although a cylinder placed in a supersonic jet is not necessarily a practical control mechanism for screech noise, it was demonstrated to be effective for screech elimination and suggests the exploration of more practical means of generating additional sound sources in the flow.

Acknowledgments

The water table was established under Australian Research Council Research Infrastructure Equipment and Facilities Scheme (RIEF) grant (R00107872).

References

- [1] Powell, A., "On the Noise Emanating from a Two-Dimensional Jet Above Critical Pressure," *The Aeronautical Quarterly*, Vol. 4, No. 2, 1953, pp. 103–122.
- [2] Ho, C. M., and Nossier, N. S., "Dynamics of an Impinging Jet, Part 1: The Feedback Phenomenon," *Journal of Fluid Mechanics*, Vol. 105, Apr. 1981, pp. 119–142.
- [3] Tam, W. C. K., "Supersonic Jet Noise," *Annual Review of Fluid Mechanics*, Vol. 27, Jan. 1995, pp. 17–43.
- [4] Brocher, E., and Makhsud, A., "A New Look at the Screech Tone Mechanism of Underexpanded Jets," *European Journal of Mechanics, B/Fluids*, Vol. 16, No. 6, 1997, pp. 877–891.
- [5] Panda, J., "An Experimental Investigation of Screech Noise Generation," *Journal of Fluid Mechanics*, Vol. 378, No. 1, 1999, pp. 71–96.
- [6] Alkislir, M. B., Krothapalli, A., and Lourenco, L. M., "Structure of a Screeching Rectangular Jet: A Stereoscopic Particle Image Velocimetry Study," *Journal of Fluid Mechanics*, Vol. 489, Aug. 2003, pp. 121–154.
- [7] Norum, T. D., "Screech Suppression in Supersonic Jets," *AIAA Journal*, Vol. 21, No. 2, 1983, pp. 235–240.
- [8] Nagel, R. T., Denham, J. W., and Papanthasiou, A. G., "Supersonic Jet Screech Tone Cancellation," *AIAA Journal*, Vol. 21, No. 11, 1983, pp. 1541–1545.
- [9] Umeda, Y., Maeda, H., and Ishii, R., "Discrete Tones Generated by the Impingement of a High-Speed Jet on a Circular Cylinder," *Physics of Fluids*, Vol. 30, No. 8, 1987, pp. 2380–2388.
- [10] Preiswerk, E., "Application of the Methods of Gas Dynamics to Water Flows with a Free Surface," *Mitteilungen der Institut für Aerodynamik*, No. 7, Eidgenössische Technische Hochschule (E.T.H.), Zurich, 1938, pp. 934–935.
- [11] Black, J., and Mediratta, O. P., "Supersonic Flow Investigations with Hydraulic Analogy Water Channel," *The Aeronautical Quarterly*, Vol. 2, Feb. 1951, pp. 227–253.
- [12] De Chant, L. J., and Caton, J. A., "Measurement of Confined Supersonic, 2-D Jet Lengths Using the Hydraulic Analogy," *Experiments in Fluids*, Vol. 24, No. 1, 1998, pp. 58–65.
- [13] Rani, S. L., and Wooldridge, M. S., "Quantitative Flow Visualization Using the Hydraulic Analogy," *Experiments in Fluids*, Vol. 28, No. 2, 2000, pp. 165–169.
- [14] Hourigan, K., Thompson, M. C., Welsh, M. C., and Brocher, E., "Acoustic Sources in a Tripped Flow Past a Resonator Tube," *AIAA Journal*, Vol. 30, No. 2, 1992, pp. 1484–1491.
- [15] Brocher, E., and Betton, E. M., "Experiments with the Hydraulic Analogy of a Shock-Wave Magneto-hydrodynamic Generator," *Physics of Fluids*, Vol. 18, No. 7, 1975, pp. 795–802.
- [16] Ponton, M. K., and Seiner, J. M., "The Effects of Nozzle Exit Lip Thickness on Plume Resonance," *Journal of Sound and Vibration*, Vol. 154, No. 3, 1992, pp. 531–549.
- [17] Lebedev, M. G., "Linear Solutions for the Emission of Screech Tone in Supersonic Jets," *Computational Mathematics and Modeling*, Vol. 14, No. 2, 2003, pp. 135–148.
- [18] White, F. M., *Fluid Mechanics*, 4th ed., McGraw-Hill, Singapore, 1999.
- [19] Krothapalli, A., Hsia, Y., Baganoff, D., and Karamecheti, K., "The Role of Screech Tones in Mixing of an Underexpanded Rectangular Jet," *Journal of Sound and Vibration*, Vol. 106, No. 1, 1986, pp. 119–143.
- [20] Raman, G., "Cessation of Screech in Underexpanded Jets," *Journal of Fluid Mechanics*, Vol. 336, Apr. 1997, pp. 69–90.
- [21] Fouras, A., Hourigan, K., Kawahashi, M., and Hirahara, H., "An Improved Free Surface Topographic Technique," *Journal of Visualization*, Vol. 9, No. 1, 2006, pp. 49–56.

C. Bailly
Associate Editor